

## Properties of neutrinoless double beta decay nuclear matrix elements studied along isotopic chains

Tomás R. Rodríguez<sup>1,a</sup> and Gabriel Martínez-Pinedo<sup>1</sup>

<sup>1</sup>*IKP-Technische Universität Darmstadt, Schlossgartenstraße 2, 64289, Darmstadt, Germany*

**Abstract.** We use energy density functional methods to compute the nuclear matrix elements (NME) of neutrinoless double beta decay ( $0\nu\beta\beta$ ) in the Cadmium isotopic chain. The interconnected role of deformation, pairing, configuration mixing in the NMEs is discussed in the candidate  $^{116}\text{Cd}$  and extended to the whole isotopic chain. In addition, strong shell effects are found and compared to a generalized seniority model.

*Introduction:* Detection of lepton number violating processes like neutrinoless double beta decays ( $0\nu\beta\beta$ ) is one of the most promising scenarios to find physics beyond the standard model apart from the search for new physics at LHC [1]. A future measurement of such a process will help to disentangle the Majorana nature of the neutrino, its effective mass and the mass hierarchy problem, and there are several experiments running or planned to find it [1, 2]. In this process, an even-even nucleus can not energetically decay into the odd-odd neighbor but it is allowed into the even-even nucleus with two protons more and two neutron less. In the mechanism known as the exchange of a light Majorana neutrino, the  $0\nu\beta\beta$  decay rate is proportional to a phase space factor  $G_{0\nu}$ , and the square of both the effective Majorana mass  $\langle m_{\beta\beta} \rangle$  and the nuclear matrix element (NME)  $M^{0\nu}$ . The latter has to be evaluated from theoretical calculations using nuclear structure methods, e.g., quasiparticle random phase approximation (QRPA), interacting shell model (ISM), interacting boson model (IBM) or energy density functional methods (EDF) [3]. While most of these methods agree on the transition operator which describes the process, they differ in the way the initial and final nuclear wave functions are computed, and therefore, in the correlations taken into account. For realistic  $0\nu\beta\beta$  decays only a dozen of isotopes in the whole nuclear chart are plausible candidates to detect such a mode. The theoretical studies performed so far on NMEs have been focused on the analysis of those particular nuclei that are rather different from the nuclear structure point of view. Therefore, a systematic study of the NMEs along isotopic chains would help to pin down the most relevant nuclear structure dependencies of such NMEs, and, eventually, to constrain their values. This analysis can be also used to examine the differences/similarities between the methods normally used to compute the NMEs. In Ref. [4] we studied the NMEs along the Cd→Sn isotopic chain using EDF methods. In this contribution we summarize the most important results presented in that Letter and extend the results for the  $^{116}\text{Cd}$  candidate.

*Theoretical framework:* The  $0\nu\beta\beta$  nuclear matrix element can be written as the sum of Fermi (F) and Gamow-Teller (GT) components (neglecting the tensor term),  $M^{0\nu} = -(\frac{g_V}{g_A})^2 M_F^{0\nu} + M_{GT}^{0\nu}$ , where  $g_V = 1$  and  $g_A = 1.25$  are the vector and axial coupling constants. Assuming the closure

---

<sup>a</sup>e-mail: t.rodriguez@gsi.de

approximation, the intermediate odd-odd nucleus is not needed to be calculated, and each component of the NME can be expressed as the expectation value of a two-body operator  $\hat{M}_{F/GT}^{0\nu}$  between the initial and final ground states [1, 3]:

$$M_{F/GT}^{0\nu} = \langle 0_f^+ | \hat{M}_{F/GT}^{0\nu} | 0_i^+ \rangle \quad (1)$$

In the neutrino potentials used in the radial part of the operators  $\hat{M}_{F/GT}^{0\nu}$  we include nucleon finite size effects, short range correlations and higher order currents [3]. The nuclear states are calculated with the Gogny D1S functional [5] separately using the generator coordinate method (GCM) with the intrinsic axial quadrupole moment  $\beta_2$  as the generating coordinate and particle number ( $N, Z$ ) and angular momentum ( $I$ ) Hartree-Fock-Bogoliubov (HFB) projected wave functions  $|\psi^{N,Z;I=0}(\beta_2)\rangle$  as the many-body *basis*:

$$|0_1^+\rangle = \sum_{\beta_2} g_1^{I=0}(\beta_2) |\psi^{N,Z;I=0}(\beta_2)\rangle \quad (2)$$

being  $g_1^{I=0}(\beta_2)$  the coefficients of the expansion. The lowest energy solutions of the resulting Hill-Wheeler-Griffin equations deduced from this ansatz are variational approaches to the initial and final ground states. Hence, any observable and transition can be eventually computed within this framework (see Ref. [4] and References therein for details). In particular, this method is able to describe properly ground state binding energies for the Cd and Sn isotopes calculated in this work [4]. Finally triaxial deformed states are not taken into account because increases prohibitively the computational time and for Cd and Sn chains no major effects are expected.

**Results:** We start with analyzing the main characteristics of the NMEs in a single case, namely,  $^{116}\text{Cd}$  which is the only suitable candidate to detect  $0\nu\beta\beta$  decay in the Cd isotopic chain [1]. In Fig. 1(a)-(b) we represent the initial and final collective wave functions, i.e., the probability of finding a given deformation in those states ( $|F(\beta_2)|^2$ ). We observe that the  $^{116}\text{Cd}$  is slightly more prolate deformed while the  $^{116}\text{Sn}$  has prolate and oblate components giving a spherical nucleus in average, as it should correspond to its semi magic character. In both cases, the most relevant deformations

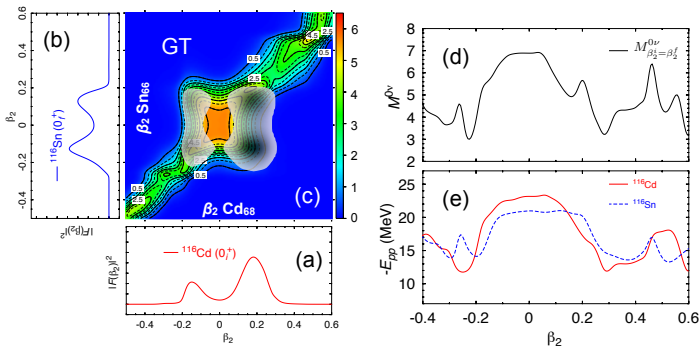


**Figure 1.** Collective wave functions for (a)  $^{116}\text{Cd}$  and (b)  $^{116}\text{Sn}$ . (c) GT-NME as a function of the initial and final quadrupole deformation ( $M_{\beta_2^i, \beta_2^f}^{0\nu} = \frac{\langle \psi^{N,Z;I=0}(\beta_2^i) | \hat{M}^{0\nu} | \psi^{N,Z;I=0}(\beta_2^f) \rangle}{\sqrt{\langle \psi^{N,Z;I=0}(\beta_2^i) | \psi^{N,Z;I=0}(\beta_2^i) \rangle \langle \psi^{N,Z;I=0}(\beta_2^f) | \psi^{N,Z;I=0}(\beta_2^f) \rangle}}$ ). The shaded area corresponds to the regions explored by the collective wave functions (a) and (b). (d) Diagonal part of the NME and (e) pairing energies for initial (continuous line) and final (dotted line) states as a function of the deformation.

are enclosed in a range of  $\beta_2 \in [-0.2, 0.2]$ . In Fig. 1(c) the GT part of the NME as a function of the initial and final deformations is represented. We observe that the NME is larger when the initial and final deformations are similar and also close to the spherical shapes. In fact, the largest value is found at  $\beta_2^i = \beta_2^f = 0$  ( $M_{\beta_2^i=\beta_2^f=0}^{0\nu} = 6.9$ ). However, the region explored by the actual wave functions (represented by the shaded area in Fig. 1(c)) excludes the spherical point -the collective wave function of  $^{116}\text{Cd}$  has a negligible weight at  $\beta_2 = 0$ - and the final NME is reduced ( $M_{\text{EDF}}^{0\nu} = 4.8$ , to be compared with two QRPA values  $M_{\text{QRPA}}^{0\nu} = 2.9$  and 4.8 and with the IBM one,  $M_{\text{IBM}}^{0\nu} = 2.8$  [3]). Apart from the reduction of the spherical NME when deformation and configuration mixing are included in the calculation, we observe a clear correlation between the pairing content of the initial and final wave functions separately and the NME value. This can be seen in Figs. 1(d)-(e) where the maxima and minima found in the diagonal part of the NME as a function of the deformation ( $M_{\beta_2^i=\beta_2^f}^{0\nu}$ ) correspond also to maxima and minima in the pairing energy ( $E_{pp}$ ) of those states.

We now extend the study of the NME calculated in one single nucleus to the whole isotopic chain  $^A\text{Cd} \rightarrow ^A\text{Sn}$ . Although  $^{116}\text{Cd}$  could only eventually decay, the study of the NMEs of such *fake* decays could shed light on the role of deformation and pairing in a more systematic manner and help to identify possible shell effects. In Fig. 2(a) the values of the NMEs for initial neutron number  $N = 50 - 84$  calculated with the full configuration mixing and only at the spherical point are represented. In both cases, a parabolic global trend is obtained, with the smallest values corresponding to the shell closures. We notice a sudden increase for  $A = 98$  case which corresponds to the decay between mirror nuclei. The large value is due to the fact that the initial and final wave functions are almost identical. As it was observed in the individual case, the NMEs are reduced from their spherical values when the quadrupole degree of freedom is explored. Larger (smaller) reductions are obtained when the differences between the initial and final mean deformation  $\bar{\beta}_2$  are larger (smaller), as we can see in Fig. 2(b). Here, Sn isotopes are in average spherical along the isotopic chain due to the  $Z = 50$  shell closure while Cd isotopes develop a slight prolate deformation away from the neutron shell closures. The relation between the NME and the pairing correlations as a function of the deformation observed in Figs. 1(c)-(d) for a single decay can be also generalized to the isotopic chain. The parabolic shape in the pairing energies of the initial and final states (see Fig. 2(c)) resembles the overall behavior

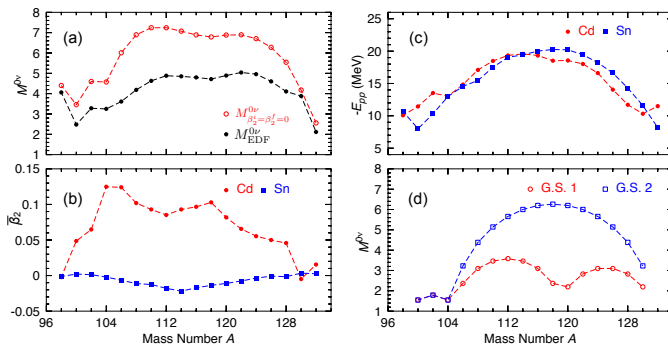


**Figure 2.** (a) NMEs calculated in the spherical point and including shape mixing along the Cd → Sn chain. (b) Mean value of the quadrupole deformation and (c) pairing energies calculated for the ground state wave functions in Cd and Sn isotopic chains. (d) Results of the generalized seniority model considering the following set of neutron shells:  $(d_{5/2}) - (g_{7/2}, s_{1/2}, d_{3/2}) - (h_{11/2})$  (G.S.1) and  $(d_{5/2}) - (g_{7/2}, s_{1/2}, d_{3/2}, h_{11/2})$  (G.S.2).

of the NMEs. We finally discuss the possible shell effects that can appear in the NMEs. Apart from the special case of the mirror decay mentioned above, we observe some fine structure in the NMEs that could be related to the role of the different shells involved. Hence, the local maxima (minima) found at  $A = 102, 112, 122$  ( $A = 104, 118$ ) could be related to the subsequent filling of the neutron  $2d_{5/2}, 1g_{7/2} - 2d_{3/2} - 3s_{1/2}$  and  $1h_{11/2}$  sub-shells. In Fig. 2(d) we represent the results of the generalized seniority model given in Eq. [46] of Ref. [6] for two different sets of single particle states, namely, G.S. 1 and 2, depending on whether the  $1h_{11/2}$  level is considered separated from the ( $gds$ ) shells. Comparing Figs. 2(a)-(d) we observe that those shell effects are present in the EDF calculation, obtaining qualitatively a similar behavior to the G.S. 1 model. Nevertheless, there is some mixture of the  $h_{11/2}$  around  $A = 120$  which produces a shallower minimum than the one found in the G.S. 1. This could also correspond to a more similar behavior to the G.S. 2 model around these points.

*Summary:* We have analyzed the role of shape mixing and pairing correlations in the  $0\nu\beta\beta$  decay nuclear matrix elements not only in the candidate  $^{116}\text{Cd}$  but also in the whole Cd isotopic chain. We have found that the main conclusions obtained for a single decay can be extended to the whole isotopic chain, i.e., larger NMEs are obtained when a) only spherical shapes are considered; b) the smaller is the difference between the deformations of the initial and final nuclei; c) the larger are the pairing correlations in the initial and final states. In addition, we have observed an enhancement in the mirror decay. Finally, we have studied the shell effects present in the NMEs and compared to the generalized seniority model.

This work was supported by the Helmholtz International Center for FAIR within the framework of the LOEWE program launched by the State of Hesse, by the Deutsche Forschungsgemeinschaft through contract SFB 634 and by the BMBF-Verbundforschungsprojekt number 06DA7047I.

## References

- [1] T. Tomoda, Rep. Prog. Phys. 54, 53 (1991); F. T. Avignone, S. R. Elliot, J. Engel, Rev. Mod. Phys. 80, 481 (2008).
- [2] H. V. Klapdor-Kleingrothaus *et al.*, Phys. Lett. B 586, 198 (2004); M. Auger *et al.*, Phys. Rev. Lett. 109, 032505 (2012); A. Gando *et al.*, Phys. Rev. Lett. 110, 062502 (2013); M. Agostini *et al.*, arXiv:1307.4720 (2013); K.-H. Ackermann *et al.*, Eur. Phys. J. C 73, 2330 (2013); D. G. Phillips II *et al.*, J. Phys.: Conf. Ser. 381 012044 (2012); I. Ogawa *et al.*, J. Phys.: Conf. Ser. 375 042018 (2012); K. Zuber, Prog. Part .Nucl. Phys. 64, 267 (2010); K. Zuber *et al.*, AIP Conf. Proc. 942, 101 (2007); J. Argyriades *et al.*, Phys. Rev. C 80, 032501(R) (2009); H Bhang *et al.*, J. Phys.: Conf. Ser. 375, 042023 (2012); C. Arnaboldi *et al.*, Phys. Rev. C 78, 035502 (2008); V. Álvarez *et al.*, JINST 8, P04002 (2013);
- [3] F. Šimkovic *et al.*, Phys. Rev. C 60, 055502 (1999); F. Šimkovic *et al.*, Phys. Rev. C 77, 045503 (2008); D.-L. Fang, A. Faessler, and V. Rodin, Phys. Rev. C 83, 034320 (2011); M. Kortelainen, J. Suhonen, Phys. Rev. C 75, 051303(R) (2007); M. T. Mustonen and J. Engel, Phys. Rev. C 87, 064302 (2013); E. Caurier *et al.*, Phys. Rev. Lett. 100, 052503 (2008); J. Menéndez *et al.*, Nucl. Phys. A 818, 139 (2009); A. Neacsu, S. Stoica, and M. Horoi, Phys. Rev. C 86, 067304 (2012); J. Barea, J. Kotila, and F. Iachello, Phys. Rev. C 87, 014315 (2013); T. R. Rodríguez and G. Martínez-Pinedo, Phys. Rev. Lett. 105, 252503 (2010).
- [4] T. R. Rodríguez and G. Martínez-Pinedo, Phys. Lett. B 719, 174 (2013).
- [5] J. F. Berger *et al.*, Nucl. Phys. A **428**, 23 (1984).
- [6] J. Barea and F. Iachello, Phys. Rev. C **79**, 044301 (2009).